

Multi-agent DRL-based Lane Change Decision Model for Cooperative Planning in Mixed Traffic

Zeyu Mu¹, Shangtong Zhang² and B. Brian Park³

Abstract—Connected automated vehicles (CAVs) possess the ability to communicate and coordinate with one another, enabling cooperative platooning that enhances both energy efficiency and traffic flow. However, during the initial stage of CAV deployment, the sparse distribution of CAVs among human-driven vehicles reduces the likelihood of forming effective cooperative platoons. To address this challenge, this study proposes a hybrid multi-agent lane change decision model aimed at increasing CAV participation in cooperative platooning and maximizing its associated benefits. The proposed model employs the QMIX framework, integrating traffic data processed through a convolutional neural network (CNN-QMIX). This architecture addresses a critical issue in dynamic traffic scenarios by enabling CAVs to make optimal decisions irrespective of the varying number of CAVs present in mixed traffic. Additionally, a trajectory planner and a model predictive controller are designed to ensure smooth and safe lane-change execution. The proposed model is trained and evaluated within a microsimulation environment under varying CAV market penetration rates. The results demonstrate that the proposed model efficiently manages fluctuating traffic agent numbers, significantly outperforming the baseline rule-based models. Notably, it enhances cooperative platooning rates up to 26.2%, showcasing its potential to optimize CAV cooperation and traffic dynamics during the early stage of deployment.

Index Terms—Multi-Agent, Reinforcement Learning, Cooperative Platooning, Lane Change

I. INTRODUCTION

The rapid advancement in connected automated vehicle (CAV) technologies promises significant improvements in road safety, traffic efficiency, and energy conservation [1]. These vehicles leverage vehicle-to-vehicle (V2V) communication exchanging critical data such as speed, position, and acceleration, which enables CAVs to optimize decision-making processes and follow safely and closely to each other to improve the traffic capacity and efficiency. Cooperative adaptive cruise control (CACC) is one of the key technologies that enhances adaptive cruise control (ACC) by cooperating with its connected preceding vehicle via V2V communication and then bring benefits in terms of individual safety, comfort, energy efficiency [2]–[4], and road capacity and traffic efficiency [5], [6].

¹Zeyu Mu is with the Link Lab and Department of Systems and Information Engineering, University of Virginia, Charlottesville, VA 22903, USA (dwe4dt@wisc.edu)

³B.B. Park is with the Link Lab and Departments of Civil & Environmental Engineering and Systems & Information Engineering, University of Virginia, Charlottesville, VA 22904 USA; (bp6v@virginia.edu)

²Shangtong Zhang is with Department of Computer Science, University of Virginia, Charlottesville, VA 22903, USA (shangtong@virginia.edu)

However, in the early stage of CAV deployment, the sparse distribution of CAVs poses a limitation for CAV to communicate with its immediate CAV and then realize cooperative platooning. Therefore, CAV organization for platoon is important to investigate and improve the potential capability of CAV in mixed traffic scenarios. Many researchers [7]–[9] have proposed strategies for organizing CAVs for cooperative platooning, such as dedicated lanes for CAVs or lane changes for cooperative platooning. Dedicated lanes would be exclusively reserved for CAVs, significantly increasing the likelihood of forming cooperative platoons and thereby streamlining traffic flow [10]–[12]. However, the practicality of dedicated lanes is limited during the early stage of CAV deployment, when low market penetration rates may make exclusive CAV lanes an inefficient use of road space. Therefore, at the early stage of CAV deployment, lane changes to follow or lead another CAV in adjacent lanes offer a more flexible means for forming cooperative platoons, thereby enhancing safety, improving energy consumption over time, and optimizing space [13]–[15].

Current research on lane-change strategies for cooperative platoons often focuses on optimizing platoon formation using predefined information, such as departure times, routes, destinations, or on-demand scenarios [16]–[18]. These studies primarily emphasize small-scale truck coordination and fuel efficiency improvements during lane changes, relying on access to private information. However, for individual CAVs, which constitute the majority of traffic participants, private information is generally not shared due to privacy concerns. To address this limitation, an alternative approach prioritizes maximizing the similarity of commonly shared information, such as speed and position between CAVs [19], with lane change decisions made using a greedy optimization method. However, the greedy method is not flexible enough to handle the complexity and uncertainty of the real-world traffic.

The complexity of lane-changing behavior becomes even more pronounced in mixed traffic environments where CAVs and human-driven vehicles coexist. In such scenarios, lane changes represent a critical domain in which CAVs can influence road safety and overall traffic flow [20]. Unlike CAVs, human drivers typically make lane change decisions based on self-serving motivations, such as achieving higher speeds or accessing more space. These individualistic behaviors can disrupt traffic by forcing following vehicles to decelerate or yield, thereby undermining the efficiency gains of cooperative platooning. In addition, the presence of human drivers introduces significant randomness and uncertainty to the dynamics

of lane change, further complicating efforts to achieve smooth and efficient traffic flow. Statistically, lane changes contribute significantly to traffic accidents, with approximately 539,000 traffic accidents reported annually in the United States [21]. Addressing these challenges necessitates the development of strategies that not only balance individual vehicle incentives with the broader objective of minimizing traffic disruptions but also incorporate a deeper understanding of vehicle cooperation and human driving behavior for safety [22].

A critical tool for addressing these challenges is the lane-change decision model, which determines whether a lane change is warranted to improve driving conditions and influences surrounding traffic. Traditional research on lane changes has primarily centered on rule-based models. Gipps [23] developed lane change rules that account for a variety of factors, including safe gap distances, the presence of permanent obstructions, transit lanes, intended maneuvers by the driver, the presence of heavy vehicles, and vehicle speeds. Kesting et al. [24] introduced the Minimizing Overall Braking Induced by Lane Changes (MOBIL) principle, which incorporates a politeness parameter, aiming to encourage more cooperative behavior during lane changes. More contemporary approaches frequently assess the utility of potential lane changes [25], [26], providing a more dynamic and predictive understanding of traffic flow and driver behaviors. Rule-based models are mostly based on handcrafted rules and criteria to imitate the driving behaviors of human drivers and offer interpretability. However, as the criteria and rules behind these models are typically handcrafted, such models lack flexibility and generalization performance.

In recent years, the field of deep learning has made revolutionary progress across a wide array of domains. These advancements include image and speech recognition, natural language processing, autonomous driving, and personalized healthcare [27]. By combining deep neural networks with reinforcement learning, artificial intelligence has evolved in different domains [28]–[30]. The success of deep reinforcement learning (DRL) motivates many researchers to investigate and apply DRL to autonomous driving [31], [32]. Compared with rule-based and utility-based data-driven models, DRL-based methods can greatly decrease the heavy reliance on the large amount of data. Alternatively, DRL-based models learn and enhance their understanding and knowledge via trial-and-error. As lane change behaviors are one of the most complex driving maneuvers for vehicles, many researchers make efforts by applying DRL to lane changes, including decision-making [33]–[35] and trajectory planning [36]–[38].

Efforts to enhance the performance of DRL-based lane-change models have taken various approaches. Some researchers have focused on improving the model's input by designing sophisticated observation spaces or incorporating specific network structures to enhance input processing [39], [40]. Others have explored reward function design, creating tailored reward mechanisms to improve model performance [41], [42]. Additionally, new algorithms and frameworks for lane-change decision-making have been proposed [37], [43]–

[45]. Despite these advancements, most existing models adopt a single-agent paradigm, which overlooks the interactive nature of vehicle behaviors in traffic. This limitation results in overly simplistic models that pose significant safety risks. Furthermore, many models focus solely on optimizing the performance of the ego vehicle, neglecting collaboration with surrounding vehicles.

In dynamic traffic environments, multiple CAVs make self-interest-based lane change decisions, leading to potential conflicts that require cooperation to achieve global optimizations for both safety and traffic efficiency. To address this challenge, some researchers have incorporated multi-agent techniques, enabling CAVs to learn cooperative strategies during training. For instance, Zhang et al. [35] proposed a multi-agent lane-change decision model to enhance collaboration among CAVs by considering right-of-way and the impact of lane changes. Similarly, a study by Guo et al. [46] introduced a transformer-based deep deterministic policy gradient method for multi-agent scenarios, aiming to emulate cooperative and competitive interactions among vehicles. [47] enhanced the QMIX to be applied for CAV coordination at the non-signalized intersection. Despite advancements in multi-agent DRL-based lane-change models, several critical deficiencies remain. Firstly, in dynamic traffic environments, the number of CAVs fluctuates over time and is strongly influenced by the market penetration rate of CAVs. To the best of our knowledge, existing research mainly focuses on fixed number of agents and has not adequately addressed the challenge of enabling CAVs to make lane change decisions under varying number of agents. This gap is significant, as addressing it is crucial for solving lane-change problems in diverse traffic scenarios and as the number of vehicles varies over time in real-world traffic. Furthermore, most studies focus primarily on higher speeds or larger spaces as incentives for lane change, often neglecting the broader benefits of cooperative platooning for CAV. Specifically, when a CAV has already formed a cooperative platoon with its connected preceding vehicle, as shown in Figure 1, making a lane change to follow a traditional human-driven vehicle with a higher speed undermines the advantages of cooperative platooning. Such actions not only reduce the energy and traffic flow benefits of cooperative platooning but also introduce safety risks due to the stochastic and unpredictable nature of human-driven vehicles.

To address these challenges mentioned above, this study proposes a proactive strategy in which CAVs cooperate and execute strategic lane changes to maximize the benefits of cooperative platooning under varying market penetration rate of CAVs. To accommodate the varying number of agents and the dynamic nature of mixed-traffic environments, a hybrid multi-agent DRL-based lane-change decision framework is introduced. The framework employs CNN-QMIX for high-level lane-change decision-making and integrates an optimization-based lane-change trajectory planner with advanced controllers for safe and efficient execution. The deep CNN-QMIX model combines the strengths of convolutional neural networks (CNNs) and the QMIX algorithm to process

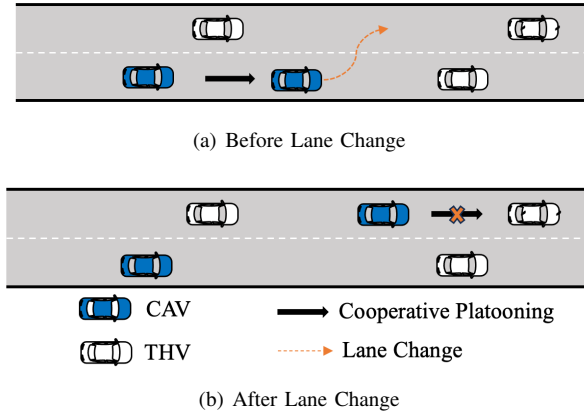


Fig. 1. Lane Change Decision for Speed Incentive and Sabotaging Cooperative Platooning

spatial and temporal data extracted from dynamic traffic snapshots. The QMIX algorithm employs centralized training and decentralized deployment, enabling CAVs to learn cooperative strategies, explore opportunities for cooperative platooning, and adapt to the stochastic behaviors of human drivers. The introduction of CNNs is to effectively extract hierarchical spatial features from high-dimensional input data across diverse visual traffic scenarios without requiring explicit programming for each case. For lane-change trajectory planning and control, the framework incorporates a reference trajectory planner and a model predictive control (MPC) scheme to ensure smooth and safe lane-change execution. Additionally, ACC and CACC controllers are utilized to support conventional following or cooperative platooning when necessary.

The key contributions of this study are summarized as follows:

- The study highlighted the limitations of speed-focused lane-change incentives in current models, particularly their failure to preserve the benefits of cooperative platooning. It proposed a novel strategy to ensure that lane changes prioritized platooning efficiency while mitigating safety risks associated with following unpredictable human-driven vehicles.
- The study tackled the challenge of fluctuating CAV numbers in dynamic traffic environments, a factor strongly influenced by varying market penetration rates. This issue, often overlooked in existing research, is crucial for addressing lane-change problems in diverse and realistic traffic scenarios.
- The study introduced a hybrid multi-agent DRL-based lane-change decision framework tailored to maximize the cooperative platooning under mixed-traffic environments. This framework combined high-level decision-making through CNN-QMIX with low-level trajectory planning and control to achieve safe and efficient execution.

This paper is organized as follows: The control framework, including the multi-agent DRL-based lane change algorithm and lane change planner and controller described in Section

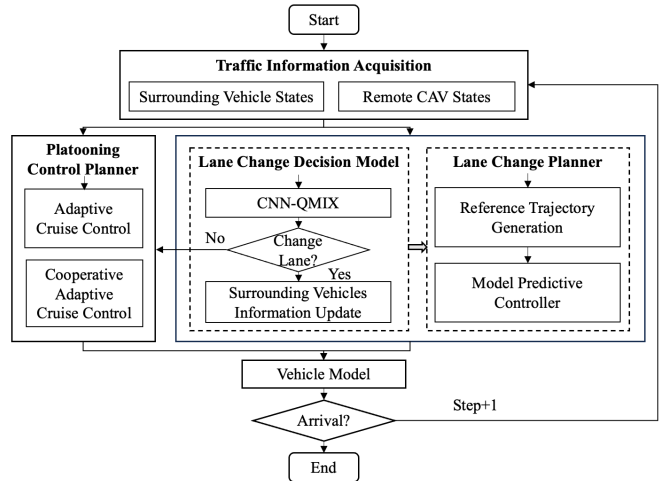


Fig. 2. Lane Change Process Overview

II. Section III gives an overview of simulation design and settings. In Section IV, the training and testing results are presented and evaluated. Finally, the conclusions and future work are given in Section V.

II. LANE CHANGE MODEL

A. Overview

The lane change process is divided into two key sections: i) lane change decision-making, and ii) trajectory planning and controlling for lane change and platooning before and after lane changes. The specific lane change implementation is shown in Fig. 2. The CAV is assumed to be equipped with a comprehensive suite of sensors and communication technologies. These systems enable the CAV to continuously acquire the states of nearby vehicles and remote CAVs, including their positions and speeds.

When the preceding vehicle is connected, the CAV activates the CACC system to optimize its car-following behavior. In scenarios where the preceding vehicle lacks connectivity, the ACC system is utilized instead. A multi-agent DRL network is employed to make lane change decisions based on real-time information about surrounding vehicles. Upon deciding to change lanes, the CAV updates its lane identification and re-calibrates the data of the surrounding vehicle. Conversely, if no lane change is initiated, the information about surrounding vehicles remains unchanged. Once a lane change decision is made, a trajectory planner generates a smooth lane change trajectory based on the initial and final states of the vehicle. The MPC system then executes the lane change by tracking the planned trajectory. This decision-making and control process is repeated iteratively at each time step until the CAV completes its journey.

B. Multi-agent Lane Change Decision Model

Reinforcement learning (RL) has gained significant attention for addressing complex decision-making problems in

multi-agent systems (MAS), especially in cooperative environments where multiple agents must work together to achieve a common goal. A widely adopted theoretical foundation for modeling such problems is the decentralized partially observable Markov decision process (DEC-POMDP). This mathematical framework captures the inherent challenges of multi-agent settings, where agents operate under partial observability. This means each agent only has access to its own local observations and history, without knowing the full state of the environment. Moreover, control is decentralized, meaning there is no central authority to dictate actions, and agents must independently decide their actions while coordinating with others to maximize a shared reward. Many multi-agent reinforcement learning (MARL) algorithms aim to approximate or learn decentralized policies that are effective under the DEC-POMDP formulation. However, the inherent non-stationarity of multi-agent environments, where each agent's policy evolves during learning, makes this problem particularly difficult. Traditional approaches like independent Q-learning often fail in these settings due to the lack of coordination among agents and the resulting instability.

In response, more advanced methods have been developed to enable effective cooperation. One prominent example is QMIX, an extension of the Deep Q-Network (DQN) framework, specifically designed for MARL tasks. QMIX leverages the paradigm of centralized training with decentralized execution (CTDE), which allows agents to benefit from global state information during training while still making decisions based solely on their local observations during deployment. This approach mitigates the non-stationarity problem by stabilizing the learning process with centralized information, while preserving the decentralized nature of execution. Compared to alternative MARL methods, such as policy-based approaches like Multi-Agent Deep Deterministic Policy Gradient (MADDPG) [48], which often require significant computational resources, QMIX offers a more scalable and sample-efficient solution. Its ability to balance coordination and efficiency makes it particularly suitable for real-world applications, such as cooperative driving in traffic scenarios, where multiple autonomous vehicles must make independent yet coordinated decisions in dynamic environments.

1) *QMIX*: In QMIX, each agent i maintains a separate Q-network $Q_i(s_i, a_i)$, which estimates the expected cumulative reward for taking action a_i in its observed state s_i . These individual Q-values are computed independently and then aggregated using a mixing network, which integrates local information into a global decision-making framework. This mixing network combines the individual Q-values into a joint action-value function Q_{total} . This function represents the overall performance of the multi-agent system and ensures that the joint Q-function is monotonically increasing with respect to each agent's individual Q-value. The mathematical formulation is shown in (1).

$$Q_{\text{total}} = f(Q_1, Q_2, \dots, Q_n) \quad (1)$$

where $f(\cdot)$ is a parameterized function that determines how the individual Q-values are combined. The mixing network is structured in such a way that its weights and biases are functions of the global state, allowing it to adapt dynamically to changing conditions. This monotonicity constraint guarantees that if an individual agent increases its Q-value, the joint Q-value also improves. As a result, decentralized execution is feasible, as each agent can make independent decisions while ensuring system-wide optimization. During deployment, each agent relies only on its local Q-network to make decisions, eliminating the need for global state access in real time.

The learning process in QMIX is guided by minimizing the Temporal Difference (TD) error, a fundamental concept in reinforcement learning that ensures convergence to an optimal Q-function. The loss function $L(\theta)$ is defined in (2).

$$L(\theta) = \mathbb{E} \left[\left(r + \gamma \max_{a'} Q_{\text{total}}(s', a'; \theta_t^-) - Q_{\text{total}}(s, a; \theta_t) \right)^2 \right] \quad (2)$$

where s represents the state, a denotes the action, and r is the reward. The term $Q_{\text{total}}(s, a; \theta_t)$ corresponds to the estimated joint Q-value for the state-action pair (s, a) parameterized by the current network θ_t . The target Q-value $r + \gamma \max_{a'} Q_{\text{total}}(s', a'; \theta_t^-)$ is computed using the highest Q-value estimate for the next states' and action a' leveraging a separate target network θ_t^- for stability. The discount factor γ , a constant between 0 and 1, controls the significance of future rewards. A lower γ prioritizes immediate rewards, making future rewards less influential, whereas a higher γ encourages long-term planning by assigning greater weight to future returns.

2) *CNN-QMIX for Varying Number of Agents*: QMIX is a widely used value-based MARL algorithm that has demonstrated effectiveness in various cooperative settings. However, one of its key limitations is its inability to handle a varying number of agents, as it is inherently designed for a fixed agent count during training. The Q-networks and mixing network are architecturally constrained to the specific number of agents used during training. If the number of agents changes dynamically, the learned model becomes incompatible with the new agent configuration. In real-world traffic scenarios, the number of vehicles dynamically changes as vehicles move out of the communication range or make turns and exit the roadway, which presents a significant challenge for QMIX.

To overcome this limitation, we propose to utilize CNN-QMIX, a novel extension of QMIX that integrates Convolutional Neural Networks (CNN) to allow the model to handle a varying number of agents efficiently. The core idea is to replace the traditional fixed-size mixing network with a more adaptive architecture capable of processing a flexible number of inputs to construct a universal network architecture for QMIX's utility functions. Instead of using a list of individual Q-values as input, we employ a grid-based state representation, where the traffic environment is represented as a spatial map. Each agent's information (e.g., position, velocity, lane status) is mapped onto a discretized grid, allowing the convolutional

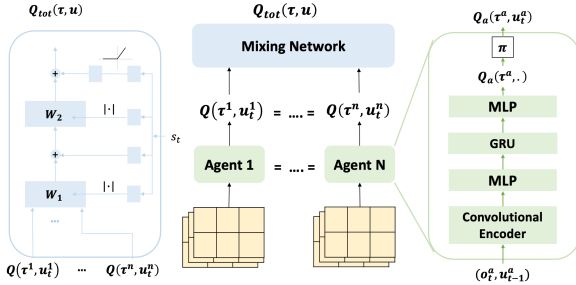


Fig. 3. The Architecture of the Multi-agent DRL-based Lane Change Decision Model

layers to process agent states independently of the number of agents. A CNN is used to process the grid input, enabling the model to learn spatial relationships between agents. This structure ensures that even as the number of agents changes, the CNN can extract meaningful features without requiring architectural modifications. The overall architecture of the proposed model is illustrated in Fig. 3.

Each agent i receives local observations (o_t^i, u_t^{i-1}) at time t from grid matrix, which include current local state information and the previous action. The agent Q-networks estimate individual action-value functions $Q_i(\tau^i, u_t^i)$ where τ^i represents the agent's trajectory. Q-values are fed into the mixing network, which computes the global Q-value Q_{total} . State information s_t is fed into the mixing network to dynamically adjust the weighting (W_i) of Q-values. The policy π selects an action u_t^a using an ϵ -greedy exploration strategy, meaning the agent explores random actions with probability ϵ .

In this study, we transform the traffic data into a grid-like matrix, allowing the use of CNN [27] to effectively extract spatial features and identify traffic patterns from the high-dimensional, image-like data. After the grid-based observation is generated, it is processed through a convolutional encoder, which extracts spatial features from the input. The encoder's output is then flattened into a one-dimensional tensor, enabling the integration of additional one-dimensional information, such as agent identifiers, the most recent action taken, and other relevant attributes. This combined representation is subsequently passed through a fully connected linear layer, followed by a Rectified Linear Unit (ReLU) activation function. Next, the network incorporates a Gated Recurrent Unit (GRU) cell [49], which captures temporal dependencies and utilizes historical time-series data to enhance decision-making. The final layer is another fully connected layer, which produces Q-values corresponding to each possible action. Conceptually, the convolutional encoder captures spatial relationships within the observation, while the fully connected layers distill this information to generate actionable insights in the form of Q-values. The GRU cell further enriches this process by leveraging temporal context, ensuring more informed and robust predictions.

In this study, CNN-QMIX is applied to a strategic lane-change decision model to optimize cooperative vehicle platooning through lane changes. The multi-agent system in this scenario consists of multiple CAVs, each acting as an independent agent. The goal is to optimize lane-change decisions for cooperative platooning while maintaining safety. The lane change decision model is defined as follows.

State Space: The model incorporates three state variables, as defined in (3). These variables include the longitudinal position x , longitudinal speed v and the type of vehicle is encoded as $\text{typ} \in \{0, 1, 2\}$, where 0 indicates the absence of a vehicle, 1 represents a human-driven vehicle, and 2 corresponds to a CAV. These state variables contain necessary information as inputs to the model.

$$s \in \{x, v, \text{type}\} \quad (3)$$

Action Space: The action space of the model consists of three discrete actions: a right lane change, maintaining the current lane, and a left lane change. These actions are encoded as $a \in \{-1, 0, 1\}$, where -1 corresponds to a right lane change, 0 denotes maintaining the current lane, and 1 represents a left lane change, as expressed in (4).

$$a \in \{-1, 0, 1\} \quad (4)$$

Reward: In the lane change decision-making process, the reward function plays a critical role in guiding the learning process by encouraging the CAV to make decisions that lead to desirable outcomes. This study considers three key factors in designing the reward function: cooperative platooning, safety, and higher speed. Safety is the primary concern in lane selection, as improper lane changes can result in rear-end or side-swipe collisions. The safety reward function evaluates whether the ego CAV maintains a safe gap from its surrounding vehicles. This is expressed in (5),

$$r_d = e^{-r \min(|(x_p - x) - h_{\min}|, |(x - x_f) - h_{\min}|)} \quad (5)$$

where $(x_p - x)$ and $(x - x_f)$ are the relative distances of the ego CAV from its preceding vehicle and following vehicle, respectively, and h_{\min} is the minimum safe distance. r is a constant to adjust the exponential function's decay rate. This function assigns higher rewards when the ego CAV maintains a larger minimum safe distance, ensuring collision avoidance. When the gap is small, the reward diminishes exponentially, discouraging unsafe lane changes.

Maintaining a desirable speed is essential for traffic efficiency, as significant deviations from the optimal speed may cause traffic disruptions and reduce fuel efficiency. The speed reward function encourages the ego CAV to maintain a velocity v close to the desired speed v_d , formulated as in (6),

$$r_v = e^{-m|v_p - v|} \quad (6)$$

where m is a constant to adjust the exponential function's decay rate. The function assigns higher rewards when the ego CAV follows a preceding vehicle that matches the desired speed. Conversely, if the speed deviation is large, the reward decreases, motivating the vehicle to switch lanes when necessary.

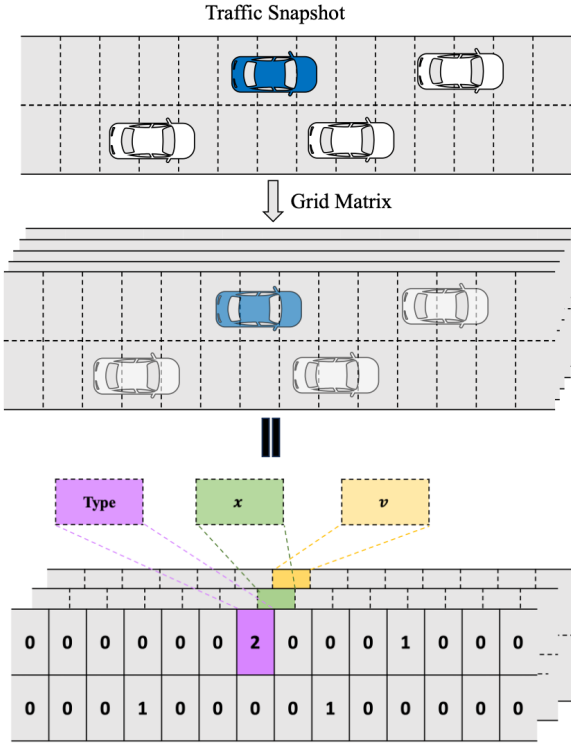


Fig. 4. The Input Process for the Multi-agent DRL-based Lane Change Decision Model

Platooning enhances fuel efficiency and traffic stability by enabling CAVs to travel in close formations with minimal speed fluctuations. To incentivize cooperative platooning, we introduce a positive reward, defined by (7), that encourages CAVs to follow another connected vehicle instead of a manually driven vehicle.

$$r_c = \max(0, \log_{10}^{2n}) \quad (7)$$

where n is the number of connected vehicles in front the agent. This function rewards higher values when the ego CAV follows a longer platoon of CAVs, fostering cooperative platooning behavior. The logarithmic transformation ensures diminishing returns when multiple connected vehicles are present, preventing excessive emphasis on this reward factor.

To reinforce safe lane-change behavior, a negative reward is applied when a collision occurs. The overall reward function is provided in (8).

$$r = \begin{cases} w_1 r_c + w_2 r_v + w_3 r_d, & \text{if no collision} \\ -5, & \text{if collision} \end{cases} \quad (8)$$

This harsh penalty discourages reckless lane changes and ensures that safety remains the highest priority in the learned policy.

Input: The input of the agent model is the surrounding traffic information and remote CAVs information within V2V communication range. The input is transformed into a 3-dimensional matrix of size $k \times n \times m$. Here, k represents

the number of information channels, n represents the number of lanes, m corresponds to the number of cells dividing the road segment, which is calculated as ratio of the sensing range length to the cell length, as shown in Fig. 4. For example, if there are two lanes, the cell length is 10 meters, and the sensing range is 100 meters, then n is 2 and m is calculated as $\frac{100}{10} = 10$. In this study, we consider three information channels, which are the states $s \in \{x, v, \text{type}\}$.

C. Lane Change Planner and Controller

MARL is efficient in high-level decision-making and cooperative behavior among CAVs, enabling system-level optimization of traffic flow, safety, and energy efficiency. However, direct execution through MARL often struggles with real-time feasibility and stability due to its sample inefficiency and lack of explicit constraint handling. Therefore, in this study, we propose to utilize MARL for lane change decision-making, while the lane change trajectory planning and execution is conducted by a trajectory planner and Model Predictive Controller (MPC). By integrating MPC for execution, the system benefits from its ability to generate dynamically feasible, constraint-satisfying, and collision-free trajectories in real time. MPC optimally refines the planned trajectory by considering vehicle dynamics, control limits, and immediate environmental changes, ensuring smooth and safe lane transitions.

The lane change trajectory planner is designed to generate a smooth and safe trajectory for the CAV to transition from one lane to another. To ensure smooth motion while minimizing acceleration and jerk to enhance passenger comfort, the cost function is minimized to determine the optimal trajectory. The cost function, C , is an integral formulation to optimize the entire trajectory from time $t = 0$ to $t = t_f$, expressed as (9),

$$\begin{aligned} \min \quad & C = \int_0^{t_f} (c_1 a^2 + c_2 J^2 + c_3 (y - y_f)^2) dt \\ \text{s.t.} \quad & \begin{cases} x(t) = a_5 t^5 + a_4 t^4 + a_3 t^3 + a_2 t^2 + a_1 t + a_0 \\ y(t) = b_5 t^5 + b_4 t^4 + b_3 t^3 + b_2 t^2 + b_1 t + b_0 \end{cases} \end{aligned} \quad (9)$$

where a^2 is the control effort (acceleration); J^2 is the jerk (rate of change of acceleration); $(y - y_f)^2$: is the deviation of current lateral positon from the final lateral position. The weights c_1, c_2 and c_3 determine the relative importance of acceleration, jerk, and lateral deviation. The vehicle's trajectory is modeled using polynomial equations. These are 5th-order polynomials, which are often used in trajectory generation because they allow smooth transitions with controlled position, velocity, acceleration, and jerk. The coefficients a_5, a_4, \dots and b_5, b_4, \dots are parameters to be optimized.

Once the trajectory is planned based on (9), a MPC controller is employed to execute the lane change while accounting for real-time disturbances and dynamic constraints. MPC is an optimization-based control method that predicts the vehicle's future states over a finite horizon and determines the optimal control inputs (e.g., steering and acceleration) to follow the desired trajectory while respecting physical constraints, such as actuator limits and collision avoidance.

MPC continuously updates its predictions and control actions in real time, making it robust and adaptive to dynamic traffic scenarios. In this study, the MPC controller is designed to ensure stable and precise movements from the planned trajectory in the longitudinal and lateral directions. The controller minimizes a quadratic cost function as shown in (10).

$$\begin{aligned} \min_{w, b, \xi} \quad & \sum_0^N (r_n - Y_n)^T Q (r_n - Y_n) + \sum_0^N \Delta u_n^T R \Delta u_n \\ \text{s.t.} \quad & u_{\min} \leq u \leq u_{\max} \\ & X_{n+1} = AX_n + B\Delta u_n \\ & Y = CX_n \end{aligned} \quad (10)$$

where N is the prediction horizon, r is the reference trajectory from the planner, and Y is the predicted trajectory of the vehicle (the actual trajectory estimated based on current vehicle dynamics). Δu represents changes in control inputs (steering and acceleration adjustments), and Q, R are weight matrices to penalize deviations from the reference trajectory and large control efforts, respectively. Additionally, X is the state vector of position, velocity, and acceleration, and u is the control input vector of acceleration and steering; A is the state matrix and B is the control input matrix. Matrices A and B are determined from the vehicle model.

The vehicle model in this study follows a kinematic bicycle model $\dot{x} = f(x, u)$ that includes an additional, assumed response delay between the commanded and realized acceleration [50].

$$\dot{x} = v \cos(\theta + \beta) \quad (11a)$$

$$\dot{y} = v \sin(\theta + \beta) \quad (11b)$$

$$\dot{v} = a \quad (11c)$$

$$\dot{a} = (u_a - a)/\tau \quad (11d)$$

$$\dot{\theta} = (v/L_r) \sin \beta \quad (11e)$$

This model includes the algebraic relation of the angle of the velocity vector deviated from the longitudinal axis of the vehicle

$$\beta = \arctan \left(\frac{L_r}{L_r + L_f} \tan u_\delta \right),$$

and parameters τ as the first-order lag constant between the commanded and realized forward acceleration, and L_f, L_r as the lengths of the vehicle mass center to the front and rear axles, respectively.

The current vehicle state (X) and the control input (Δu) matrices at time step n are given by:

$$X = \begin{bmatrix} x \\ y \\ \theta \\ v \\ a \end{bmatrix}, \quad u(n) = \begin{bmatrix} u_a \\ u_\delta \end{bmatrix}.$$

where the global fixed-frame coordinates x, y , the respective heading angle θ , as well as the forward velocity v and acceleration a are collected as states of the vehicle. The inputs

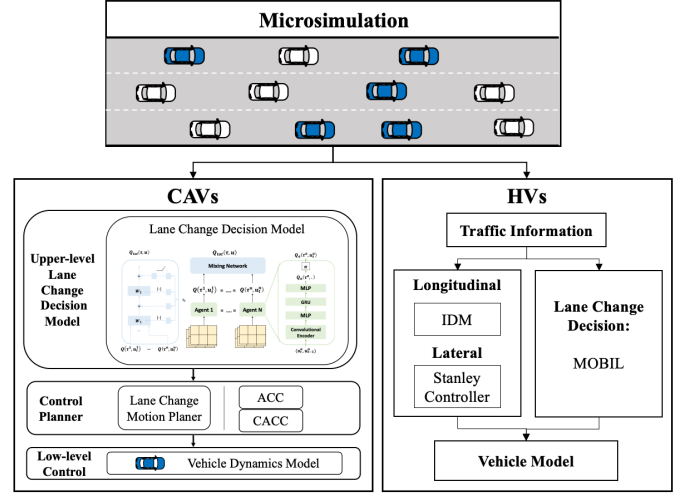


Fig. 5. Microsimulation Framework

from longitudinal and lateral vehicle controls of commanded acceleration u_a and steering angle u_δ are collected as vehicle input. The matrices A and B are given based on the vehicle model, defined as,

$$A = \begin{bmatrix} 0 & 0 & 0 & 1 & 0 \\ 0 & 0 & v_0 & 0 & 0 \\ 0 & 0 & 0 & 0 & 0 \\ 0 & 0 & 0 & 0 & 1 \\ 0 & 0 & 0 & 0 & -1/\tau \end{bmatrix}, \quad B = \begin{bmatrix} 0 & 0 \\ 0 & 0.5v_0 \\ 0 & \frac{v_0}{2L_r} \\ 0 & 0 \\ \frac{1}{\tau} & 0 \end{bmatrix}.$$

During the updated phase, the Kalman Filter (KF) determines the Kalman gain and updates the predicted state $x(n+1)$ and covariance error of the system using the current measurement input $\Delta u(k)$.

III. MICROSIMULATION SETUP

A microsimulation framework is implemented using Python to model vehicle interactions and efficiently generate training data for the agents. The structure of the microsimulation is illustrated in Fig. 5. The simulation environment consists of a three-lane, 1200-meter road segment. 24 vehicles are randomly generated in the starting area of the road and travel through 1200-meter road segment. The proportion of CAVs within this setup is determined by the MPR of CAVs.

To assess the effectiveness of the proposed multi-agent DRL-based lane change decision model in promoting cooperative platooning among CAVs, the positions of the vehicles are randomly generated in three lanes. The widely-used MOBIL (Minimizing Overall Braking Induced by Lane Changes) model [51] and a decentralized greedy method designed for cooperative platooning as two rule-based baselines for the proposed lane change decision model. The HVs only employ the MOBIL model for lane change decisions. Additionally, the Intelligent Driver Model (IDM) [52] is used for longitudinal control in HVs. A detailed explanation of the baseline rule-

based lane change decision model, the baseline longitudinal control, and the vehicle model is provided below.

A. Baseline Lane Change Models

1) *MOBIL Model for Rule-Based Lane Change*: The MOBIL model acts as a rule-based baseline lane selection model [51]. Each lane change direction $\Delta\gamma \in \{1, -1, 0\}$ to the left, to the right, and to maintain the current lane, are considered feasible only if the following constraint criteria hold true.

$$a' - a > p(a_r - a'_r) [\gamma > 1] + p(a_{r'} - a'_{r'}) + \Delta a_t \quad (12a)$$

$$a'_{r'} > -b_s \quad (12b)$$

$$t - t_\ell > \Delta t_\ell \quad (12c)$$

In the case of multiple feasible lanes, the lane that maximizes the following utility is then selected [51].

$$a' - a + p(a_r - a'_r) [\gamma > 1] + p(a_{r'} - a'_{r'}) + a_b [\Delta\gamma = -1] \quad (13)$$

Here, a is the commanded ego vehicle acceleration, a_r is the rear vehicle acceleration as evaluated according to (21), and ' indicates respective terms that would result after a lane change occurs (for example, $a'_{r'}$ is the acceleration that the new rear vehicle would follow if the ego changed into their lane.)

Additionally, the quantity $t - t_\ell$ is the time since a previous lane change occurred for the ego vehicle or any nearby neighboring vehicle, $\Delta t_\ell = 8\text{ s}$ is the threshold before a new lane change is allowed, $p = 0.10$ is a politeness factor, $\Delta a_t = 0.20 \text{ m/s}^2$ is an acceleration threshold, $b_s = 0.80 \text{ m/s}^2$ is a safe admissible braking deceleration, and $a_b = 0.20 \text{ m/s}^2$ is a lane direction bias that adds utility only if considering to change towards the right lane.

2) *Decentralized Greedy Lane Change Decision Model for Cooperative Platooning*: Compared to MOBIL, which primarily considers safety, speed, and politeness, the greedy lane change decision model [19] incorporates the individual properties of vehicles during assignment computation. This approach enables the optimization of platooning benefits at the level of individual vehicles.

To achieve this, the desired driving speed is used as the primary similarity metric. Additionally, the spatial position of vehicles on the freeway is also factored into the assignment process. The assignment is represented by a matrix A , defined as a $|C| \times |T|$ matrix containing a decision variable a_{ij} for each potential vehicle-to-platoon assignment between elements of C (searching vehicles) and T (potential platoons or vehicles). The decision variable a_{ij} is defined as follows:

$$a_{ij} = \begin{cases} 1, & \text{if } c_i \text{ is assigned to } t_j, \\ 0, & \text{otherwise.} \end{cases} \quad (14)$$

If a searching vehicle c_i cannot be assigned to any other vehicle or platoon t_j (where $c_i \neq t_j$), it will continue driving individually. This scenario is modeled as a self-assignment, where $a_{ii} = 1$ with $c_i = t_j$. Consequently, every searching vehicle c_i in the assignment matrix A has an assignment. It is

important to note that A is generally asymmetric, and not all assignments between c_i and t_j are feasible (as detailed below).

To quantify the similarity between vehicles and potential platoons, we define a similarity matrix F , also of dimension $|C| \times |T|$. Each element f_{ij} represents the similarity (or deviation) between the properties of c_i and t_j , computed as:

$$f(c, t) = \alpha \cdot d_s(c, t) + (1 - \alpha) \cdot d_p(c, t), \quad \alpha \in [0, 1], \quad (15)$$

where $\alpha \in [0, 1]$ is a weighting coefficient balancing the contributions of the desired speed deviation $d_s(c, t)$ and the position deviation $d_p(c, t)$, which are defined as follows:

$$d_s(c, t) = \frac{|D_c - D_t|}{m \cdot D_c}, \quad m \in [0, 1], \quad (16)$$

$$d_p(c, t) = \frac{\min(|p_c - p_t|, |l_t - p_c|)}{r}, \quad r \in \mathbb{N}, \quad (17)$$

Here, $d_s(c, t)$ measures the normalized deviation in desired driving speed between vehicle c and target t , where m represents the maximum allowed deviation from the desired speed. Similarly, $d_p(c, t)$ calculates the normalized deviation in position on the freeway, with r representing the maximum allowable search range for candidate assignments. Both equations (16) and (17) compute deviations that collectively define the similarity metric in Equation (15).

B. Longitudinal Automated Control for Cooperative Platooning

Adaptive Cruise Control (ACC) [53] is an advanced driver assistance system designed for longitudinal control in automated vehicles. Its primary objectives are to improve driving comfort and enhance energy efficiency. ACC systems operate by utilizing the measured motion of the preceding vehicle to control the subject vehicle, ensuring that a safe following gap is maintained. In this study, a commonly used proportional-derivative (PD) controller is implemented to model the behavior of ACC systems. The control input, $u(t)$, is defined in terms of the spacing error, $e(t)$, as given by Eq. (19).

$$u(t) = k_p e(t) + k_d \dot{e}(t) \quad (18)$$

Here, k_p and k_d are the proportional and derivative gains of the controller, respectively. The spacing error, $e(t)$, represents the difference between the desired gap ($h_d(t)$) and the actual gap at time t . The desired gap is calculated as $h_d(t) = v(t) \cdot T + s_0$, where $v(t)$ is the current speed, T is the desired time headway, and s_0 is the standstill distance.

However, when an ACC-equipped vehicle follows an unconnected vehicle at a short desired time headway, disturbances, such as abrupt deceleration by the lead vehicle, can cause oscillations. These oscillations may propagate along the vehicle platoon, amplifying the disturbance. This raises safety concerns, as such dynamics can lead to congestion and, in extreme cases, collisions [54].

TABLE I
INTELLIGENT DRIVER MODEL PARAMETERS.

Symbol	Description	Value
a_0	maximum acceleration	1.52 [m/s ²]
b_0	comfortable deceleration	3.24 [m/s ²]
T	desired headway	1.02 [s]
v_0	desired velocity	15.4 [m/s]
s_0	desired standstill distance	6.0 [m]
δ	acceleration exponent	4.0 [-]

To address these limitations, Cooperative Adaptive Cruise Control (CACC) [53] was developed to enhance ACC performance by incorporating Vehicle-to-Vehicle (V2V) communication and forming cooperative platoons. The additional acceleration information transmitted by the connected preceding vehicle allows the CACC system to mitigate disturbances through a designed feed-forward filter. This feed-forward filter uses the acceleration of the connected preceding vehicle as an input signal to stabilize the system.

Similar to the ACC system, the acceleration command $u(t)$ in the CACC system is expressed using the same PD controller formulation in Eq. (19), augmented with a feed-forward filter $f(\cdot)$ that is designed based on a zero-error condition, as described in Eq. (20).

$$u(t) = k_p e(t) + k_d \dot{e}(t) + f(a(t)) \quad (19)$$

$$f(a(t)) = [\tau(-\frac{e^{-\frac{t}{T}}}{T^2} + \frac{1}{T}) + \frac{e^{-\frac{t}{T}}}{T}]a(t) \quad (20)$$

For both ACC and CACC systems, the parameters used in this study are $k_p = 0.5$, $k_d = 0.3$, as specified in [53].

C. Human Driver Longitudinal Modeling

The Intelligent Driver Model (IDM) acts as a car-following model for the native microsimulated vehicles [52]. The model commands acceleration as a function of velocity, v , and the relative gap and velocity difference from its preceding vehicle, Δs and Δv

$$a_{\text{IDM}} = a_0 \left(1 - \left(\frac{v}{v_0} \right)^\delta - \left(\frac{s^*(v, \Delta v)}{\Delta s} \right)^2 \right) \quad (21)$$

with the target distance function

$$s^*(v, \Delta v) = s_0 + \max \left\{ 0, T v + \frac{v \Delta v}{2\sqrt{a_0 b_0}} \right\}.$$

Here, a_0 is the maximum acceleration, b_0 is the comfortable deceleration, s_0 is the desired standstill gap, v_0 is the desired velocity, δ is a velocity-error exponent, and T is the desired time headway. Table I lists the parameters for the IDM used in the simulation experiments as based on [55] to replicate human driving patterns.

TABLE II
PARAMETER SETTINGS FOR LANE-CHANGE DECISION MODEL

Symbol	Definition	Value
L_{tail}	Tail perception range	100 m
L_{head}	Forward perception range	100 m
L_{grid}	Width of the snapshot's grid	10 m
\bar{T}_D	Length of the predicted trajectory	2 s
w_1	Weight for R_1	1
w_2	Weight for R_2	0.5
w_3	Weight for R_3	2
λ	Learning rate	0.0001
Ψ	Experience memory pool size	5000
B	Batch of transitions size	128
γ	Discount factor	0.5

D. Simulation and Training Settings

To train and evaluate the lane-change strategy for cooperative platooning proposed in this study, we develop a multi-lane highway traffic environment using the simulator described in Section III. The simulator is designed to emphasize the driving behavior characteristics of automated vehicles. The proposed strategy is deployed within this simulation environment, where all vehicles are capable of making lane-change decisions independently.

In the simulation, we implement a multi-agent deep reinforcement learning (DRL)-based lane-change decision model that integrates lane-change planning, control, and automated coordination to enable cooperative platooning among CAVs. In contrast, HVs operate based on the IDM for longitudinal control and the MOBIL model for lane-change decisions. The proportions of CAVs and HVs in the traffic environment are determined by the MPR of CAVs, which is varied across three levels: 12.5%, 37.5%, and 50%. It is important to note that the simulation focuses on the early deployment phase of CAVs. During this phase, the proposed model prioritizes maximizing the probability of CAVs forming cooperative platoons, even when opportunities to encounter other CAVs are limited. This design ensures that the model addresses challenges specific to sparse CAV environments, where forming platoons is more difficult but highly beneficial for traffic efficiency and energy savings. This simulation setup allows for a comprehensive evaluation of the proposed strategy's effectiveness in mixed traffic scenarios. By varying the MPR, we can assess the model's ability to optimize CAV behavior, ensure safety, and improve overall traffic performance under diverse traffic compositions.

The hyperparameters for the proposed lane change decision models, including the number of layers, neurons per layer, learning rate, and activation functions, were manually tuned through empirical testing and grid-based exploration to achieve optimal performance. For different types of layers and units, the ranges were set as [1, 5] and [32, 64, 128, 256], respectively. The hyperparameters are summarized in Table II, while the architecture of the neural network is detailed in Table III. The training process spans a total of 100,000 episodes. Model parameters are saved every 200 episodes, and

TABLE III
NEURAL NETWORK LAYOUT FOR OUR LANE-CHANGE DECISION MODEL

Layer	Parameters
CNN Layer 1	Patch size = (3, 3), stride = (2, 2), number of filters = 16, activation = ReLU
CNN Layer 2	Patch size = (3, 3), stride = (2, 2), number of filters = 32, activation = ReLU
CNN Layer 3	Patch size = (2, 2), stride = (1, 2), number of filters = 16, activation = ReLU
FC Layer 1&2	Number of units = 128, activation function = ReLU
FC Layer 3&4	Number of units = 64, activation function = ReLU

the parameters corresponding to the highest observed rewards are saved immediately. The implementation of the models utilizes the PyTorch framework. During each episode, the initial positions of the vehicles are randomly assigned within the range of [100, 300] meters, while all other parameters are set according to the desired configurations outlined in Table I.

IV. EVALUATION AND ANALYSIS

A. Performance Metrics

Based on the reward function proposed in Section II, the performance objectives for the lane-change decision model focus on optimizing the behavior of CAV within cooperative platooning. The goals are to enhance energy efficiency and traffic flow while ensuring safety and minimizing unnecessary lane changes, which can cause traffic disturbances and reduce overall system efficiency.

To comprehensively evaluate the performance of our lane-change decision model, we consider five key metrics: platoon rate, number of lane changes, average speed, collision rate, and energy consumption. The platoon rate measures the percentage of CAVs successfully participating in cooperative platooning. A higher platoon rate indicates effective coordination among vehicles, which enhances corresponding benefits. The total number of lane changes performed by all vehicles is recorded to evaluate their impact on traffic flow stability. While lane changes are necessary for achieving optimal platoon formation and avoiding conflicts, excessive lane changes can introduce turbulence in traffic, disrupt flow, and increase the likelihood of accidents. The average speed of all vehicles is calculated to assess traffic efficiency. Higher average speeds without compromising safety suggest that the system effectively optimizes vehicle behavior to maintain smooth and efficient traffic flow. Energy consumption for all vehicles is computed as the integral of acceleration over time, reflecting changes in vehicle speed and their impact on energy use. This metric provides insights into whether the proposed model improves energy efficiency by optimizing acceleration and deceleration patterns during cooperative platooning.

B. Training of the Lane Change Decision Model

Based on the microsimulation framework and training settings detailed in Section III, the DRL-based lane change

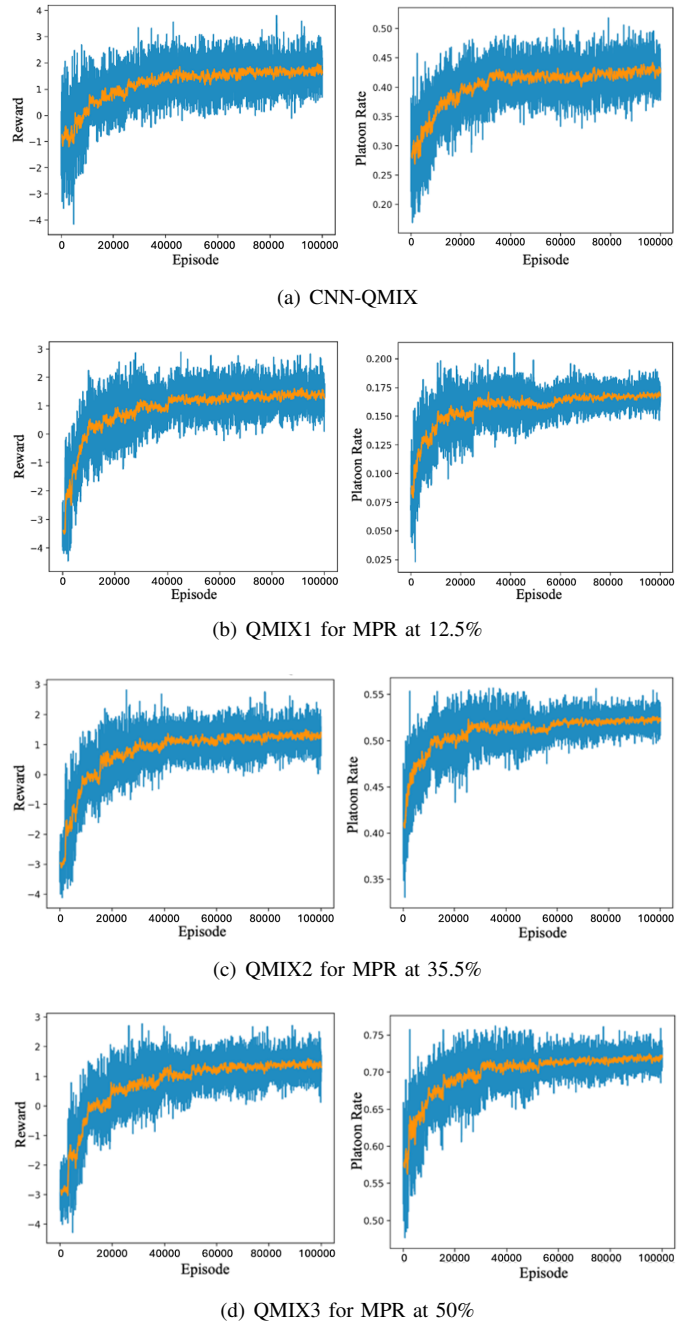


Fig. 6. Training results of Multi-agent DRL-based lane change decision model, including reward and platoon rate (blue line is the moving average of 10 episodes, and orange line is moving average of 100 episodes)

decision model was trained to achieve the objectives specified in the reward function. The results shown in this section require running the training continuously for 24 hours.

To assess whether the proposed lane change decision model can effectively handle dynamically changing agents, both the proposed CNN-QMIX and the baseline QMIX were trained for comparison. Unlike CNN-QMIX, QMIX requires prior knowledge of the number of agents in the traffic, necessitating separate models for each MPR. Specifically, for MPRs of

12.5%, 37.5%, and 50.0%, three separate models, QMIX1, QMIX2, and QMIX3, were trained to enable CAVs to make lane-changing decisions under each respective scenario. In contrast, CNN-QMIX is inherently designed to handle dynamically changing agent populations in traffic. This allows it to be trained as a single model applicable across varying MPRs, making it more flexible and scalable for real-world applications where traffic conditions are highly variable.

The comparative training outcomes of the QMIX and CNN-QMIX models across varying MPRs are illustrated in Figure 6. The CNN-QMIX model demonstrates a robust performance, characterized by a relatively stable reward metric that shows minor fluctuations, generally maintaining an average level around 1.5. Concurrently, the platoon rate exhibits a progressive increase, stabilizing approximately at 0.5. This performance indicates that the CNN-QMIX model effectively manages the dynamic fluctuations in the number of CAVs and facilitates efficient platoon formation across different MPRs without necessitating multiple model configurations.

In contrast, the traditional QMIX model requires separate training instances for each MPR, revealing a model that is less adaptable to changes in traffic density. Although QMIX is capable of converging in terms of reward and platoon rate, it necessitates a longer training duration as the number of CAVs increases. This model also displays a pronounced initial volatility in reward metrics, which eventually stabilizes. In comparison, CNN-QMIX shows a more gradual increase in both reward and platoon rate metrics, taking more time to reach convergence. This slower convergence rate can be attributed to the CNN-QMIX model's integration of CNNs and its exposure to a broader range of scenarios during training. Such extensive training allows the agent to learn more about cooperative behaviors and make more informed lane-changing decisions, though it requires more time to assimilate and optimize these behaviors effectively.

Overall, the CNN-QMIX's ability to handle dynamically changing agent populations not only highlights its flexibility and scalability but also underscores its suitability for real-world applications where traffic conditions are highly variable. This adaptability makes it a preferred model over traditional QMIX in environments requiring robust response capabilities to fluctuating traffic densities.

C. Test Evaluation

Using the trained CNN-QMIX model with the highest reward, we conducted 100 test simulations in the same microsimulation environment, with initial vehicle positions randomly generated for each test. Table IV presents a performance comparison between QMIX and CNN-QMIX under different MPRs during the early deployment phase of CAVs.

For QMIX, the best-performing models were selected separately for each MPR: QMIX1, QMIX2, and QMIX3, corresponding to models trained under MPRs of 12.5%, 37.5%, and 50.0%, respectively. In contrast, CNN-QMIX was trained across varying MPRs, providing a generalized model capable of adapting to different penetration levels. This distinction

TABLE IV
PERFORMANCE COMPARISON FOR DIFFERENT METHODS UNDER VARYING MARKET PENETRATION RATES.

MPR	Method	Platoon Rate	Max Length	Time [s]	LC
12.5%	QMIX1	0.20	1.8	48	2.8
	CNN-QMIX	0.21	1.9	52	2.7
37.5%	QMIX2	0.50	3.5	34	3.6
	CNN-QMIX	0.53	3.4	35	3.7
50.0%	QMIX3	0.70	4.8	28	3.1
	CNN-QMIX	0.72	4.9	29	3.0

highlights the flexibility of CNN-QMIX in mixed traffic scenarios, where the MPR of CAVs may vary dynamically. Result comparisions can underscore the robustness of CNN-QMIX in handling varying MPRs during early CAV deployment.

As shown in Table IV, both QMIX and CNN-QMIX demonstrate an increase in platoon rates as the MPR of CAVs rises. At 12.5%, the platoon rates are relatively low (0.20 for QMIX and 0.21 for CNN-QMIX), reflecting the difficulty of forming platoons when the density of CAVs is limited. However, at higher MPRs of 37.5% and 50.0%, the platoon rates increase significantly. CNN-QMIX consistently achieves higher platoon rates than QMIX across all MPR levels, albeit with marginal gains, such as a 1% improvement at 12.5% and a 2% improvement at 50.0%. In terms of maximum platoon length, CNN-QMIX slightly outperforms QMIX at each MPR level, indicating that the convolutional layers in CNN-QMIX enhance spatial awareness, enabling the formation of larger and more cohesive platoons. However, this advantage comes with a minor trade-off. The time required to form platoons is slightly longer for CNN-QMIX at 12.5% and 37.5%, suggesting that the model prioritizes forming larger and more stable platoons. Notably, this difference becomes negligible at 50.0%, where both models demonstrate comparable performance. When evaluating the number of lane changes, CNN-QMIX exhibits slightly fewer lane changes than QMIX at 12.5% and 50.0%, suggesting an improvement in decision-making efficiency. Nevertheless, the differences in lane-change frequency between the two models are not substantial.

Overall, these results indicate that CNN-QMIX consistently outperforms QMIX across key metrics, including platoon rates, maximum platoon length, and decision-making efficiency, albeit with modest improvements. Importantly, the findings suggest that QMIX is capable of effectively managing varying numbers of agents in traffic scenarios, maintaining robust performance even when trained under a range of MPRs rather than being tailored to specific MPR conditions. This highlights the model's adaptability and generalization capabilities in dynamic traffic environments.

We subsequently compare rule-based lane-change decision models, including the MOBIL and greedy methods described in Section III. It is important to note that MOBIL is primarily designed to prioritize speed incentives and safety. Consequently, it may leave cooperative platoons to pursue higher

TABLE V

PERFORMANCE COMPARISON FOR RULED-BASED MODELS (MOBIL, GREEDY, GREEDY (RLC)), AND CNN-QMIX UNDER VARYING MARKET PENETRATION RATES.

MPR	Method	Platoon Rate	Max Length	Time [s]	LC
12.5%	MOBIL	0.10	1.1	N/A	3.1
	Greedy	0.16	1.4	46	2.1
	Greedy (RLC)	0.18	1.5	74	2.7
	CNN-QMIX	0.21	1.9	52	2.7
37.5%	MOBIL	0.30	1.8	N/A	3.5
	Greedy	0.42	2.5	33	2.9
	Greedy (RLC)	0.43	2.8	49	3.6
	CNN-QMIX	0.53	3.4	35	3.7
50%	MOBIL	0.52	2.8	N/A	3.9
	Greedy	0.62	3.1	33	2.5
	Greedy (RLC)	0.65	3.2	38	3.1
	CNN-QMIX	0.72	4.9	29	3.0

speeds, similar to conventional lane-change models, thereby limiting its ability to support long-term platooning. In contrast, the greedy method is specifically designed to facilitate platoon formation but remains constrained by handcrafted rules, which may not fully capture the complexities of dynamic traffic scenarios. The results, presented in Table V, highlight the significant advantages of learning-based approaches, such as CNN-QMIX, over traditional rule-based strategies. It is worth noting that the greedy method generally results in fewer lane changes compared to CNN-QMIX. To determine if these more lane changes contribute to more cooperative platooning, we introduce a random lane-change (RLC) mechanism based on the MOBIL model, which provides CAVs with additional opportunities to explore and engage in cooperative platooning. This random lane change is permitted only when the number of lane changes performed by the greedy method is lower than that observed with CNN-QMIX.

As shown in Table V, all methods demonstrate a consistent increase in platoon rates as the MPR of CAV rises. Notably, this trend is observed even for the MOBIL model, which is not explicitly designed for cooperative platooning. This finding underscores the enhanced opportunities for platoon formation as the density of CAVs increases. Among the methods evaluated, CNN-QMIX consistently achieves the highest platoon rates and maximum platoon lengths across all MPR levels, highlighting its superior capability to facilitate cooperative behavior among CAVs.

At an MPR of 12.5%, CNN-QMIX achieves the highest platoon rate, representing a 110% improvement over MOBIL, a 21.3% improvement over Greedy, and a 16.7% improvement over Greedy (RLC). These results demonstrate CNN-QMIX's effectiveness in promoting platoon formation even in sparse CAV scenarios, where coordination is inherently more challenging. The performance gap widens at an MPR of 35.5%, where CNN-QMIX outperforms MOBIL by 76.7%,

Greedy by 26.2%, and Greedy (RLC) by 23.3%. As the MPR of CAVs increases to 50%, CNN-QMIX achieves a platoon rate of 0.72, which is 38.5% higher than MOBIL, 26.1% higher than Greedy, and 20.8% higher than Greedy (RLC). This trend indicates that CNN-QMIX is particularly effective at improving platoon rates in low to moderate MPR scenarios.

However, the relative improvement of CNN-QMIX diminishes slightly as the MPR increases to higher levels, where many CAVs are already capable of forming cooperative platoons. In contrast, the performance of MOBIL is significantly worse than other methods in terms of platoon rate, as MOBIL is primarily designed to prioritize speed incentives and safety rather than cooperative platooning. For the greedy method, the number of platoons formed is lower even when random lane changes are permitted to match the frequency of lane changes in the CNN-QMIX method. This indicates that the Greedy approach lacks the necessary coordination to maximize platoon formation. A similar trend is observed in the maximum platoon length, where CNN-QMIX consistently outperforms the other methods. Moreover, CNN-QMIX generally requires less time to form platoons, particularly as the MPR of CAVs increases, further highlighting its efficiency in facilitating cooperative behaviors among CAVs.

TABLE VI
PERFORMANCE COMPARISON OF CONNECTED AUTOMATED VEHICLES USING MOBIL, GREEDY, AND CNN-QMIX UNDER VARYING MARKET PENETRATION RATES.

MPR	Method	Mean Speed	Energy Consumption
12.5%	MOBIL	30.1	203
	Greedy	29.1	188
	CNN-QMIX	31.0	182
37.5%	MOBIL	31.3	199
	Greedy	30.4	180
	CNN-QMIX	32.9	175
50%	MOBIL	32.8	193
	Greedy	32.0	175
	CNN-QMIX	34.0	162

We conducted a comprehensive analysis of both energy efficiency and traffic efficiency (measured by mean speed) for CNN-QMIX and the rule-based baseline methods, as presented in Table VI. The results reveal that CNN-QMIX delivers notable improvements in mean speed across all MPRs. For instance, at an MPR of 37.5%, CNN-QMIX achieves a 5.1% higher mean speed compared to MOBIL and an 8.2% increase relative to Greedy. These findings underscore CNN-QMIX's ability to enhance traffic efficiency by leveraging intelligent lane-changing strategies and coordinated decision-making mechanisms.

In addition to improving traffic efficiency, CNN-QMIX demonstrates significant energy savings. At an MPR of 50%, the algorithm reduces energy consumption by 16.1% compared to MOBIL and by 7.4% relative to Greedy. This dual optimization, achieving higher mean speeds while reducing

energy consumption, highlights CNN-QMIX's capacity to balance traffic flow efficiency and energy sustainability, making it a promising approach for deployment in connected and autonomous traffic systems.

V. CONCLUSIONS AND FUTURE WORK

In this study, a novel multi-agent lane-change strategy for cooperative platooning was proposed, utilizing a high-level multi-agent deep reinforcement learning (DRL) based decision model that accommodates a dynamically varying number of agents. Our approach significantly enhanced the collaboration performance of lane-change maneuvers in cooperative platooning environments through three distinct innovations:

Firstly, we developed a multi-agent DRL-based lane-change decision model tailored to the intricate dynamics of automated driving for CAVs within traffic systems, which has not been investigated in existing research. Unlike existing models such as QMIX, which do not account for the dynamic variability in agent count, our model maintained robust performance across varying MPRs of CAVs, thereby ensuring effective adaptation to more realistic traffic scenarios. Comparative analyses demonstrated that our proposed model did not suffer performance degradation and effectively facilitates collaborative behavior in multi-agent settings.

Moreover, we devised a sophisticated reward function that not only prioritizes speed and safety but also explicitly incorporates elements of cooperative platooning. This function played a pivotal role in evaluating and enhancing the impact of collaboration among CAVs. Our experimental results revealed that the proposed model substantially surpassed the existing MOBIL and greedy algorithms in achieving higher platoon rates, thereby significantly boosting the likelihood of platoon formation even at lower MPRs of CAVs.

Finally, the implementation of an MPC controller at the execution phase of lane-change decisions ensured safety and efficiency by tracking the intended trajectory and adjusting to potential conflicts promptly. The dual-level integration of MPC with our DRL model not only guaranteed the safety of maneuvers but also contributed to the seamless execution of strategic lane changes. These enhancements proved our model as a versatile framework applicable to other behavioral planning tasks in automated vehicle systems, potentially elevating overall vehicular performance.

Despite the successes achieved, this study acknowledges two primary limitations that pave the way for future research. Currently focused on highway scenarios, our model requires adaptations to address more complex environments such as urban arterial with intersections. Future work should involve refining the reward function and model structure to enhance robustness across a broader range of traffic situations. Additionally, the parameters of our model, including the reward function, are presently configured manually. Going forward, we aim to develop these parameters as learnable attributes within the model, allowing for automated adjustments by well-trained agents, thus reducing the reliance on manual calibration. In-depth studies addressing these limitations are planned,

promising to further the capabilities of DRL applications in automated vehicular systems.

REFERENCES

- [1] D. Tian, G. Wu, K. Boriboonsomsin, and M. J. Barth, "Performance measurement evaluation framework and co-benefit tradeoff analysis for connected and automated vehicles (cav) applications: A survey," *IEEE Intelligent Transportation Systems Magazine*, vol. 10, no. 3, pp. 110–122, 2018.
- [2] K. C. Dey, L. Yan, X. Wang, Y. Wang, H. Shen, M. Chowdhury, L. Yu, C. Qiu, and V. Soundararaj, "A review of communication, driver characteristics, and controls aspects of cooperative adaptive cruise control (cacc)," *IEEE Transactions on Intelligent Transportation Systems*, vol. 17, no. 2, pp. 491–509, 2016.
- [3] S. T. Kaluva, A. Pathak, and A. Ongel, "Aerodynamic drag analysis of autonomous electric vehicle platoons," *Energies*, vol. 13, no. 15, 2020. [Online]. Available: <https://www.mdpi.com/1996-1073/13/15/4028>
- [4] J. He, Z. Tang, X. Fu, S. Leng, F. Wu, K. Huang, J. Huang, J. Zhang, Y. Zhang, A. Radford, L. Li, and Z. Xiong, "Cooperative connected autonomous vehicles (cav): Research, applications and challenges," in *2019 IEEE 27th International Conference on Network Protocols (ICNP)*, 2019, pp. 1–6.
- [5] L. Xiao, M. Wang, W. Schakel, and B. van Arem, "Unravelling effects of cooperative adaptive cruise control deactivation on traffic flow characteristics at merging bottlenecks," *Transportation Research Part C: Emerging Technologies*, vol. 96, pp. 380–397, 2018. [Online]. Available: <https://www.sciencedirect.com/science/article/pii/S0968090X1830528X>
- [6] H. Liu, X. D. Kan, S. E. Shladover, X.-Y. Lu, and R. E. Ferlisi, "Modeling impacts of cooperative adaptive cruise control on mixed traffic flow in multi-lane freeway facilities," *Transportation Research Part C: Emerging Technologies*, vol. 95, pp. 261–279, 2018. [Online]. Available: <https://www.sciencedirect.com/science/article/pii/S0968090X18310313>
- [7] K. Ma and H. Wang, "Influence of exclusive lanes for connected and autonomous vehicles on freeway traffic flow," *IEEE Access*, vol. 7, pp. 50 168–50 178, 2019.
- [8] S. Woo and A. Skabardonis, "Flow-aware platoon formation of connected automated vehicles in a mixed traffic with human-driven vehicles," *Transportation Research Part C: Emerging Technologies*, vol. 133, p. 103442, 2021. [Online]. Available: <https://www.sciencedirect.com/science/article/pii/S0968090X21004307>
- [9] L. Zhou, T. Ruan, K. Ma, C. Dong, and H. Wang, "Impact of cav platoon management on traffic flow considering degradation of control mode," *Physica A: Statistical Mechanics and its Applications*, vol. 581, p. 126193, 2021. [Online]. Available: <https://www.sciencedirect.com/science/article/pii/S0378437121004660>
- [10] S. Razmi Rad, H. Farah, H. Taale, B. van Arem, and S. P. Hoogendoorn, "Design and operation of dedicated lanes for connected and automated vehicles on motorways: A conceptual framework and research agenda," *Transportation Research Part C: Emerging Technologies*, vol. 117, p. 102664, 2020. [Online]. Available: <https://www.sciencedirect.com/science/article/pii/S0968090X20305799>
- [11] H. Chen, F. Wu, K. Hou, and T. Z. Qiu, "Leveraging dynamic right-of-way allocation and tolling policy for cav dedicated lane management to promote cav and improve mobility," *IEEE Transactions on Intelligent Transportation Systems*, pp. 1–10, 2024.
- [12] Z. Yao, L. Li, W. Liao, Y. Wang, and Y. Wu, "Optimal lane management policy for connected automated vehicles in mixed traffic flow," *Physica A: Statistical Mechanics and its Applications*, vol. 637, p. 129520, 2024. [Online]. Available: <https://www.sciencedirect.com/science/article/pii/S0378437124000281>
- [13] J. A. Laval and C. F. Daganzo, "Lane-changing in traffic streams," *Transportation Research Part B: Methodological*, vol. 40, no. 3, pp. 251–264, 2006. [Online]. Available: <https://www.sciencedirect.com/science/article/pii/S019126150500055X>
- [14] D. Chen and S. Ahn, "Capacity-drop at extended bottlenecks: Merge, diverge, and weave," *Transportation Research Part B: Methodological*, vol. 108, pp. 1–20, 2018. [Online]. Available: <https://www.sciencedirect.com/science/article/pii/S0191261517306938>
- [15] H. Liu, S. E. Shladover, X.-Y. Lu, and X. D. Kan, "Freeway vehicle fuel efficiency improvement via cooperative adaptive cruise control," *Journal of Intelligent Transportation Systems*, vol. 25, no. 6, pp. 574–586, 2021. [Online]. Available: <https://www.sciencedirect.com/science/article/pii/S1547245022003176>

[16] K.-Y. Liang, J. Mårtensson, and K. H. Johansson, "Heavy-duty vehicle platoon formation for fuel efficiency," *IEEE Transactions on Intelligent Transportation Systems*, vol. 17, no. 4, pp. 1051–1061, 2016.

[17] A. K. Bhoopalam, N. Agatz, and R. Zuidwijk, "Planning of truck platoons: A literature review and directions for future research," *Transportation Research Part B: Methodological*, vol. 107, pp. 212–228, 2018. [Online]. Available: <https://www.sciencedirect.com/science/article/pii/S0191261517305246>

[18] Y. Zeng, M. Wang, and R. T. Rajan, "Decentralized coordination for truck platooning," *Computer-Aided Civil and Infrastructure Engineering*, vol. 37, no. 15, pp. 1997–2015, 2022. [Online]. Available: <https://onlinelibrary.wiley.com/doi/abs/10.1111/mice.12899>

[19] J. Heinovski and F. Dressler, "Where to decide? centralized vs. distributed vehicle assignment for platoon formation," 2023.

[20] Z. Wang, X. Shi, and X. Li, "Review of Lane-Changing Maneuvers of Connected and Automated Vehicles: Models, Algorithms and Traffic Impact Analyses," *Journal of the Indian Institute of Science*, vol. 99, no. 4, pp. 589–599, Dec. 2019. [Online]. Available: <https://doi.org/10.1007/s41745-019-00127-7>

[21] D. Hs, "Analysis of lane-change crashes and near-crashes," 2009. [Online]. Available: <https://api.semanticscholar.org/CorpusID:172779614>

[22] X. Li and J.-Q. Sun, "Studies of vehicle lane-changing dynamics and its effect on traffic efficiency, safety and environmental impact," *Physica A: Statistical Mechanics and its Applications*, vol. 467, pp. 41–58, 2017. [Online]. Available: <https://www.sciencedirect.com/science/article/pii/S0378437116306380>

[23] P. Gipps, "A model for the structure of lane-changing decisions," *Transportation Research Part B: Methodological*, vol. 20, no. 5, pp. 403–414, 1986. [Online]. Available: <https://www.sciencedirect.com/science/article/pii/0191261586900123>

[24] A. Kesting, M. Treiber, and D. Helbing, "General lane-changing model mobil for car-following models," *Transportation Research Record*, vol. 1999, no. 1, pp. 86–94, 2007. [Online]. Available: <https://doi.org/10.3141/1999-10>

[25] K. Singh and B. Li, "Estimation of traffic densities for multilane roadways using a markov model approach," *IEEE Transactions on Industrial Electronics*, vol. 59, no. 11, pp. 4369–4376, 2012.

[26] D. Lin, L. Li, and S. E. Jabari, "Pay to change lanes: A cooperative lane-changing strategy for connected/automated driving," *Transportation Research Part C: Emerging Technologies*, vol. 105, pp. 550–564, 2019. [Online]. Available: <https://www.sciencedirect.com/science/article/pii/S0968090X18310945>

[27] L. Alzubaidi, J. Zhang, A. J. Humaidi, A. Al-Dujaili, Y. Duan, O. Al-Shamma, J. Santamaría, M. A. Fadhel, M. Al-Amidie, and L. Farhan, "Review of deep learning: concepts, CNN architectures, challenges, applications, future directions," *Journal of Big Data*, vol. 8, no. 1, p. 53, Mar. 2021. [Online]. Available: <https://doi.org/10.1186/s40537-021-00444-8>

[28] V. Mnih, K. Kavukcuoglu, D. Silver, A. A. Rusu, J. Veness, M. G. Bellemare, A. Graves, M. Riedmiller, A. K. Fidjeland, G. Ostrovski, S. Petersen, C. Beattie, A. Sadik, I. Antonoglou, H. King, D. Kumaran, D. Wierstra, S. Legg, and D. Hassabis, "Human-level control through deep reinforcement learning," vol. 518, no. 7540, pp. 529–533. [Online]. Available: <https://doi.org/10.1038/nature14236>

[29] D. Silver, J. Schrittwieser, K. Simonyan, I. Antonoglou, A. Huang, A. Guez, T. Hubert, L. Baker, M. Lai, A. Bolton, Y. Chen, T. Lillicrap, F. Hui, L. Sifre, G. van den Driessche, T. Graepel, and D. Hassabis, "Mastering the game of go without human knowledge," vol. 550, no. 7676, pp. 354–359. [Online]. Available: <https://doi.org/10.1038/nature24270>

[30] D. Silver, T. Hubert, J. Schrittwieser, I. Antonoglou, M. Lai, A. Guez, M. Lanctot, L. Sifre, D. Kumaran, T. Graepel, T. Lillicrap, K. Simonyan, and D. Hassabis, "Mastering chess and shogi by self-play with a general reinforcement learning algorithm," 2017. [Online]. Available: <https://arxiv.org/abs/1712.01815>

[31] S. Shalev-Shwartz, S. Shammah, and A. Shashua, "Safe, multi-agent, reinforcement learning for autonomous driving," 2016. [Online]. Available: <https://arxiv.org/abs/1610.03295>

[32] A. E. Sallab, M. Abdou, E. Perot, and S. Yogamani, "Deep reinforcement learning framework for autonomous driving," *Electronic Imaging*, vol. 29, no. 19, p. 70–76, Jan. 2017. [Online]. Available: <http://dx.doi.org/10.2352/ISSN.2470-1173.2017.19.AVM-023>

[33] J. Wang, Q. Zhang, D. Zhao, and Y. Chen, "Lane change decision-making through deep reinforcement learning with rule-based constraints," in *2019 International Joint Conference on Neural Networks (IJCNN)*, 2019, pp. 1–6.

[34] W. Wang, T. Qie, C. Yang, W. Liu, C. Xiang, and K. Huang, "An intelligent lane-changing behavior prediction and decision-making strategy for an autonomous vehicle," *IEEE Transactions on Industrial Electronics*, vol. 69, no. 3, pp. 2927–2937, 2022.

[35] J. Zhang, C. Chang, X. Zeng, and L. Li, "Multi-agent drl-based lane change with right-of-way collaboration awareness," *IEEE Transactions on Intelligent Transportation Systems*, vol. 24, no. 1, pp. 854–869, 2023.

[36] T. Shi, P. Wang, X. Cheng, C.-Y. Chan, and D. Huang, "Driving decision and control for automated lane change behavior based on deep reinforcement learning," in *2019 IEEE Intelligent Transportation Systems Conference (ITSC)*, 2019, pp. 2895–2900.

[37] J. Peng, S. Zhang, Y. Zhou, and Z. Li, "An integrated model for autonomous speed and lane change decision-making based on deep reinforcement learning," *IEEE Transactions on Intelligent Transportation Systems*, vol. 23, no. 11, pp. 21 848–21 860, 2022.

[38] G. Li, Y. Yang, S. Li, X. Qu, N. Lyu, and S. E. Li, "Decision making of autonomous vehicles in lane change scenarios: Deep reinforcement learning approaches with risk awareness," *Transportation Research Part C: Emerging Technologies*, vol. 134, p. 103452, 2022. [Online]. Available: <https://www.sciencedirect.com/science/article/pii/S0968090X21004411>

[39] Y. Chen, C. Dong, P. Palanisamy, P. Mudalige, K. Muelling, and J. M. Dolan, "Attention-based hierarchical deep reinforcement learning for lane change behaviors in autonomous driving," in *2019 IEEE/CVF Conference on Computer Vision and Pattern Recognition Workshops (CVPRW)*, 2019, pp. 1326–1334.

[40] J. Wang, Q. Zhang, and D. Zhao, "Highway lane change decision-making via attention-based deep reinforcement learning," *IEEE/CAA Journal of Automatica Sinica*, vol. 9, no. 3, pp. 567–569, 2022.

[41] W. Yuan, M. Yang, Y. He, C. Wang, and B. Wang, "Multi-reward architecture based reinforcement learning for highway driving policies," in *2019 IEEE Intelligent Transportation Systems Conference (ITSC)*, 2019, pp. 3810–3815.

[42] G. Wang, J. Hu, Z. Li, and L. Li, "Harmonious lane changing via deep reinforcement learning," *IEEE Transactions on Intelligent Transportation Systems*, vol. 23, no. 5, pp. 4642–4650, 2022.

[43] B. Mirchevska, C. Pek, M. Werling, M. Althoff, and J. Boedecker, "High-level decision making for safe and reasonable autonomous lane changing using reinforcement learning," in *2018 21st International Conference on Intelligent Transportation Systems (ITSC)*, 2018, pp. 2156–2162.

[44] X. Xu, L. Zuo, X. Li, L. Qian, J. Ren, and Z. Sun, "A reinforcement learning approach to autonomous decision making of intelligent vehicles on highways," *IEEE Transactions on Systems, Man, and Cybernetics: Systems*, vol. 50, no. 10, pp. 3884–3897, 2020.

[45] M. U. Yavas, T. Kumbasar, and N. K. Ure, "A real-world reinforcement learning framework for safe and human-like tactical decision-making," *IEEE Transactions on Intelligent Transportation Systems*, vol. 24, no. 11, pp. 11 773–11 784, 2023.

[46] H. Guo, M. Keyvan-Ekbatani, and K. Xie, "Modeling coupled driving behavior during lane change: A multi-agent transformer reinforcement learning approach," *Transportation Research Part C: Emerging Technologies*, vol. 165, p. 104703, 2024. [Online]. Available: <https://www.sciencedirect.com/science/article/pii/S0968090X24002249>

[47] Z. Guo, Y. Wu, L. Wang, and J. Zhang, "Coordination for connected and automated vehicles at non-signalized intersections: A value decomposition-based multiagent deep reinforcement learning approach," *IEEE Transactions on Vehicular Technology*, vol. 72, no. 3, pp. 3025–3034, 2023.

[48] R. Lowe, Y. Wu, A. Tamar, J. Harb, P. Abbeel, and I. Mordatch, "Multi-agent actor-critic for mixed cooperative-competitive environments," 2020. [Online]. Available: <https://arxiv.org/abs/1706.02275>

[49] A. Sherstinsky, "Fundamentals of recurrent neural network (rnn) and long short-term memory (lstm) network," *Physica D: Nonlinear Phenomena*, vol. 404, p. 132306, 2020. [Online]. Available: <https://www.sciencedirect.com/science/article/pii/S0167278919305974>

[50] J. Kong, M. Pfeiffer, G. Schildbach, and F. Borrelli, "Kinematic and dynamic vehicle models for autonomous driving control design," in *2015 IEEE Intelligent Vehicles Symposium (IV)*, 2015, pp. 1094–1099.

[51] A. Kesting, M. Treiber, and D. Helbing, "General lane-changing model mobil for car-following models," *Transportation Research*

Record, vol. 1999, no. 1, pp. 86–94, 2007. [Online]. Available: <https://doi.org/10.3141/1999-10>

[52] M. Treiber, A. Hennecke, and D. Helbing, “Congested traffic states in empirical observations and microscopic simulations,” *Phys. Rev. E*, vol. 62, pp. 1805–1824, Aug 2000. [Online]. Available: <https://link.aps.org/doi/10.1103/PhysRevE.62.1805>

[53] G. Naus, R. Vugts, J. Ploeg, M. Molengraaf, van de, and M. Steinbuch, “String-stable cacc design and experimental validation, a frequency-domain approach,” *IEEE Transactions on Vehicular Technology*, vol. 59, no. 9, pp. 4268–4279, 2010.

[54] M. Shang and R. E. Stern, “Impacts of commercially available adaptive cruise control vehicles on highway stability and throughput,” *Transportation Research Part C: Emerging Technologies*, vol. 122, p. 102897, 2021. [Online]. Available: <https://www.sciencedirect.com/science/article/pii/S0968090X2030797X>

[55] M. Pourabdollah, E. Bjärkvik, F. Fürer, B. Lindenberg, and K. Burgdorf, “Calibration and evaluation of car following models using real-world driving data,” in *2017 IEEE 20th International Conference on Intelligent Transportation Systems (ITSC)*, 2017, pp. 1–6.